ZULFAQAR Journal of Defence Science, Engineering & Technology
e-ISSN: 2773-5281
Vol. 7, Issue 2 (2024)
DOI: https://doi.org/10.58247/jdset-2024-0702-11
Journal homepage: https://zulfaqarjdset.upnm.edu.my

EXPLORING THE IMPACT OF DUAL ORIFICE AIR COLUMN ORIENTATIONS ON THE PRIMARY CONVERSION EFFICIENCY OF BACKWARD BENT DUCT BUOY

Nurul Afiqah Mohd Azhar[a], Mohamad Alif Omar[b], Mohd Rosdzimin Abdul Rahman[a], Azfarizal Mukhtar[b], Mohd Kamarul Huda Samion[c], Yasutaka Imai[d], Mohd Rashdan Saad[a*]

[a] Faculty of Engineering, National Defence University of Malaysia, Sungai Besi Camp, 57000 Kuala Lumpur, Malaysia
[b] Department of Mechanical Engineering, Universiti Tenaga Nasional (UNITEN), Putrajaya Campus, Jalan IKRAM-UNITEN, 43000 Kajang, Selangor Darul Ehsan, Malaysia
[c] National Water Research Institute of Malaysia (NAHRIM), Jalan Putra Permai, 43300 Seri Kembangan, Selangor Darul Ehsan, Malaysia
[d] Institute of Ocean Energy, Saga University, Saga, Japan

ARTICLE INFO

ARTICLE HISTORY
Received: 01-07-2024
Revised: 15-08-2024
Accepted: 31-10-2024
Published: 31-12-2024

KEYWORDS
Renewable energy
Ocean energy
Wave energy converter (WEC)
Oscillating water column (OWC)
Backward Bent Duct buoy (BBDB)

ABSTRACT

This research investigates the Backward Bent Duct Buoy (BBDB), a floating type of Oscillating Water Column (OWC), focus on assessing the influence of dual orifice air column orientations on its primary conversion efficiency. A significant research gap exists regarding the design of the device, particularly the orifice area at the top panel of the device, highlighting the need for more studies in this area. The problem statement emphasizes that optimizing orifice design is crucial for maximizing BBDB efficiency. The study includes the design and fabrication process of the top panel, conducted through SolidWorks CAD software and laser cutting methods using acrylic sheets as materials. Experimental results from tests conducted in a 3D wave basin at NAHRIM revealed that Configuration 1 demonstrates the highest efficiency at 0.092%, followed by Configuration 2 at 0.091%, and Configuration 3 at 0.083%. Notably, findings indicate that a longer distance between orifices contributed to higher efficiencies. These findings contribute to understanding the performance differences of BBDB configurations, offering understanding for further advancements in wave energy conversion systems.

1.0 INTRODUCTION

The escalating global population poses a growing demand for energy supply, primarily reliant on fossil fuels. Despite the adverse effects and environmental concerns associated with burning fossil fuels, the decline in this energy source could significantly impact various sectors. The combustion of fossil fuels has been a major contributor to climate change, global warming, the greenhouse effect, and detrimental effects on human health [1-2]. Recognizing these challenges, the imperative lies in the collective desire to transition towards cleaner and sustainable energy sources as the only viable solution.

Renewable energy derived from the ocean encompasses various forms of energy, including thermal, chemical, and mechanical sources. Examples of ocean energy technologies include Ocean Thermal Energy Conversion (OTEC), salinity gradient power (SGP) or known as blue energy, and wave energy converters (WEC) [3-5]. Ocean Thermal Energy Conversion (OTEC) is a sustainable energy technology that utilizes the temperature contrast between the ocean's warm surface water and its cold deep water to produce electricity whereas SGP harness electricity from the different concentration of salt between seawater and freshwater [6]. As for wave energy, it harnesses electricity through the kinetic energy of the waves. Among all ocean energy, WECs are considered more reliable due to the predictable and constant presence of waves [7-8]. This potential to transform wave energy into usable power has motivated many inventors, resulting in over a thousand patents filed by 1980, with that number significantly rising in the years since [9].

*Corresponding Author | Saad, M. R. | rashdan@upnm.edu.my

Wave Energy Converters (WEC) come in different forms, such as Oscillating Water Columns (OWC), point absorbers, overtopping devices, and attenuators [10-12]. Each devices have different ways of harvesting the energy from the waves. Point absorbers have the capability of producing a relatively high amount of electricity despite its design and build being the smaller compared to other type of WEC. One side of the device is anchored to the seabed whereas the other end would be moving in vertical motion. On the other hand, attenuators are placed in a direction that is parallel with the main wave direction and the wave motions that causes the motion in the joint are counteracted by hydraulic rams, which push high-pressure liquid to drive hydraulic motors. These hydraulic motors, in turn, operate an electrical generator. Meanwhile, OWC consists of a turbine, orifice, and a chamber. OWC utilize the rise and fall of water levels inside a chamber to create airflow. This airflow drives the turbines that is link to generators, resulting in the generation of electricity. OWC can be classified into two types: floating and fixed systems. The differences in these two is that the fixed type is anchored in one place, usually near the shore or coast whereas the floating are buoyant structures that move along with the waves and is moored to seabed. Examples of wave energy converters (WECs) include the Pelamis and Osprey as prominent attenuators, the AWS-3 and WaveBob as notable point absorbers, and the LIMPET (Land Installed Marine Powered Energy Transformer) as a well-known oscillating water column system, each showcasing unique methods for harnessing energy from ocean waves [13-15]. These technologies harness the continuous motion of ocean waves to generate sustainable and clean energy, offering a promising alternative to traditional fossil fuel-based sources.

The floating type of oscillating water column (OWC) holds a significant advantage as it can be maneuverer to exploit wave energy wherever it is present. This adaptability makes it a versatile solution for various locations with different wave patterns. Other than that, floating OWC typically have a simple body design and does not have any complex moving parts installed or submerged underwater which reduces the potential for underwater maintenance. This capability is also particularly valuable for islands or remote areas where consistent wave patterns may vary. An illustrative example is the Backward Bent Duct Buoy (BBDB), a floating OWC device. The BBDB has the potential to replace traditional diesel generators on islands [16]. By harnessing the power of ocean waves, it offers a cleaner and more sustainable energy source, reducing reliance on diesel generators that are both costly and environmentally unfriendly. This shift not only contributes to energy sustainability but also mitigates the environmental impact associated with the use of fossil fuels. However, the studies regarding BBDB are insufficient compared to other WECs, despite the BBDB's potential for higher energy output. According to Joubert et al. (2013), among the 172 types of Wave Energy Converters (WEC) listed, only three were classified as BBDB: the Ocean Energy (OE) buoy (OE 35), the OE Generation Platform (OE 12), and a developing 5kW floating offshore OWC from the Guangzhou Institute of Energy Conversion (GIEC) [16].

However, it's important to note that both the OE 35 and OE 12 are only quarter-scale prototype models. The OE buoy is noted for its low environmental impact, as it has no open moving parts that could potentially harm marine life. Additionally, maintenance is straightforward since the turbines and generators are situated above the water, which helps prevent corrosion and makes them easily accessible. Due to this research gap, the efficiency of the BBDB remains low. One area that is lacking in research is the orifice that is located at the top panel of the device. The orifice is connected to a turbine which plays an important role as during the oscillation of the water, the air trapped inside of the chamber would be exiting through the orifice. A proper design of the orifice is essential for maximizing the efficiency of the BBDB. Hence, this study is looking forward to exploring the impact of dual orifice air column orientations towards the primary conversion efficiency of the BBDB device.

2.0 MATERIALS AND METHODS

2.1 Design and Fabrication of Top Panel Air Column

The designing of the top panels was create using SolidWorks CAD software. The dimension of the BBDB device was shown in Figure 1 while Figure 2 shows the drawings and fabricated top panels. The dimension of the BBDB device was taken from previous studies [17-19]. As for the distance between the orifices in the BBDB configurations is determined by the size of the orifice, which has a diameter of 40 mm (denoted as 1D). In Configuration 1, the distance is set at 6 times the diameter (6D), which measures 240 mm. In Configuration 2, the orifices are spaced at 3 times the diameter (3D), equating to 120 mm. Finally, Configuration 3, the distance between the two orifices is set at 1.5 times the diameter (1.5D), resulting in 60 mm. The top panel was then fabricated using laser cutting method and the materials used were acrylic

*Corresponding Author | Saad, M. R. | rashdan@upnm.edu.my

sheets before conducting a wave tank test. All top panels had the same length of 600 mm, width of 200 mm and orifice diameter of 40 mm.

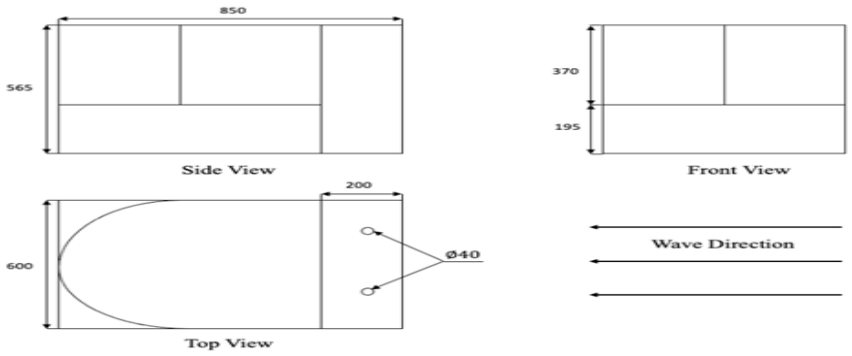

Figure 1. Dimension of BBDB from three different perspective

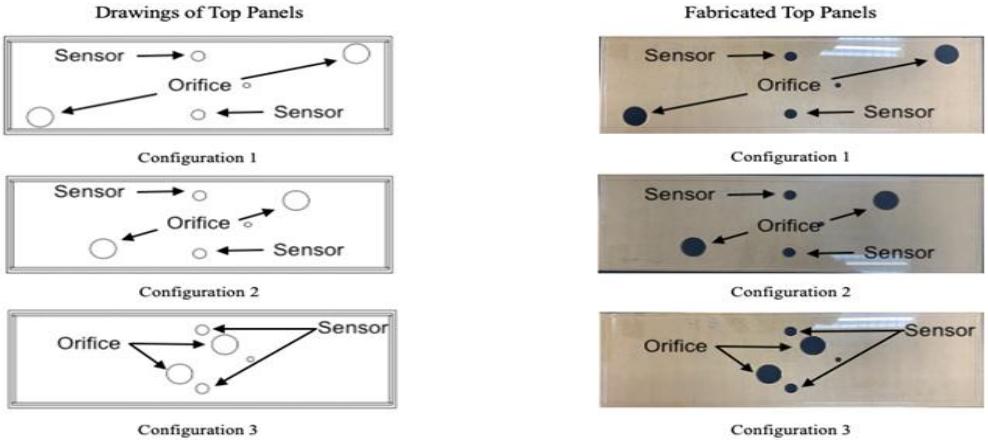

Figure 2. Fabricated Top Panels

2.2 3D Wave Basin Test

The experiment was conducted in a 3D wave basin located at the Hydraulic and Instrumentation Laboratory of the National Water Research Institute of Malaysia (NAHRIM). The dimensions of the wave basin are 30 m in length, 30 m in width, with a depth of 1.2 m and a water depth of 0.04 m as shown in Figure 3. All matters related to the management of the wave basin are handled from a control room located near the wave basin. A combination of wave periods ranging from 1 s to 3 s and a wave height of 0.1 m were used in this experiment to simulate a low heave wave condition. The chosen wave period also represents shallow water conditions, with wavelengths ranging from 0.61 to 1.843. To ensure consistency between the wave input and output, a wave probe was placed 3 m upstream from the BBDB device.

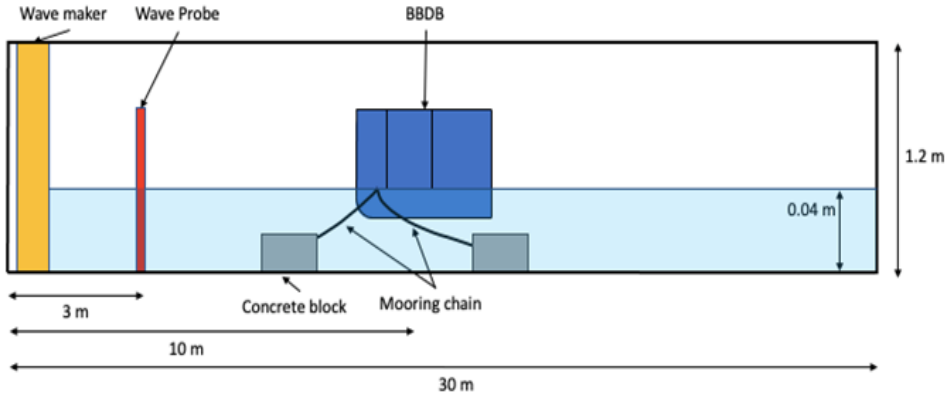

Figure 3. Schematic diagram for the experiment setup

*Corresponding Author | Saad, M. R. | rashdan@upnm.edu.my

2.3 Instrumentation

A pitot tube anemometer (EXTECH HD-350) was used in this experiment to measure the flow rate and pressure coming out of the orifice and the top view of the setup are as illustrated in Figure 4. The pressure is recorded in Pascal, and the flow rate is measured in cubic meters per minute. Subsequently, these units are converted to kilopascal and cubic meters per second, respectively, before calculating the efficiency. To enhance the stability of the Backward Bent Duct Buoy (BBDB), two steel plates, each weighing 10.5 kg, were added to the front buoy. Additionally, two mooring lines were attached to each side of the device, with a concrete block fixed to the other end, ensuring the prevention of any displacement of the BBDB during deployment.

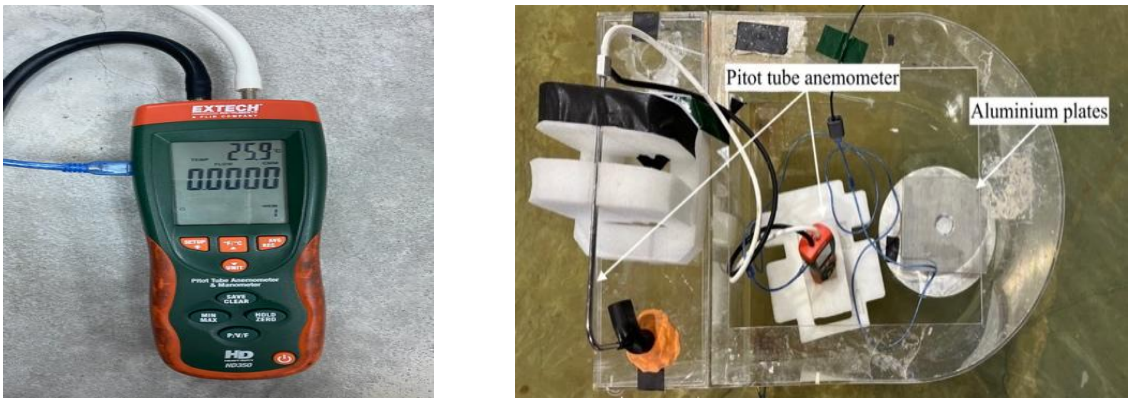

(a) (b)

Figure 4. (a) Pitot tube anemometer, (b) Top view of the device

2.4 Primary Conversion Efficiency of BBDB Device

The primary conversion efficiency of the device is determined using a formula developed by Macfarlane et al. [20]. To calculate the efficiency, both wave and air energy must be quantified. Wave energy is obtained from the incident wave, which was computed in this study using Equation (1).

$$n_1 = \frac{E_{air}}{E_{wave}} \tag{1}$$

In this study, wave energy, representing the energy obtained from incident waves, was calculated using Equation (2).

$$E_{wave} = \frac{1}{2}\rho g \zeta^2 C_g B \tag{2}$$

In Equation (2), the symbols ρ, g, B, ζ, C_g and h represent the water density (kg/m^3), gravitational acceleration (m/s^2), width of the device perpendicular to the incident wave direction (m), incident wave amplitude (m), group velocity (m/s) and water depth (m), respectively. The group velocity signifies the speed at which a wave packet travels, whereas Ω is the angular frequency of the wave (rad/s), and its equation is defined in Equation (3).

$$C_g = \frac{\Omega}{2k}\left(1 + \frac{2kh}{sinh(2kh)}\right) \tag{3}$$

As for, wave number, k represents the spatial frequency of a wave, measured in cycles per unit distance (ordinary wavenumber) as shown in Equation (4). In this context, the symbol λ represents the angular frequency of the wave measured in radians per second.

$$k = \frac{2\pi}{\lambda} \tag{4}$$

*Corresponding Author | Saad, M. R. | rashdan@upnm.edu.my

Moreover, the air energy is equivalent to the pneumatic output energy that is acquire from the orifice outlet that is located at the top panel air column. The calculation of air energy is as per Equation (5). Nevertheless, it is essential to know the pressure difference of the orifice output for a better calculation.

$$E_{air} = \frac{1}{T}\Delta P(t)Q(t)dt \tag{5}$$

The pressure difference, ΔP was obtained by subtracting the maximum and minimum pressure obtained from the orifice outlet whereas Q, the flow rate was obtained from inside the water column. Since this study uses dual orifices, the air energy from each orifice, both having the same wave period and height, was initially summed and then divided by the wave energy, as illustrated in Equation (6).

$$\Sigma E_{air} = E_{air1} + E_{air2} + \cdots + E_{airn} \tag{6}$$

3.0 RESULTS AND DISCUSSION

3.1 Pressure Amplitude in Water Column

In Figure 6, a similar fluctuating trend with three peaks is observed for all top panels. During the first peak at λ/L = 2.8, Configuration 1 exhibits the highest-pressure amplitude of 0.000257. In the second peak at λ/L = 4.3, Configuration 3 surpasses the others with the highest $P/\rho gZi$ of 0.000225, while Configuration 2 takes the lead during the third peak with a peak $P/\rho gZi$ of 0.000255. In particular, the differences between the highest and second highest $P/\rho gZi$ are minimal, with a mere 0.78% difference. This suggests that the three configurations are relatively close in performance, with each excelling in $P/\rho gZi$ during different peaks.

The increased in distance between orifice allows for more spaces where the fluid can expand and potentially increased the turbulence. This resulted in a more significant energy dissipation, leading to a higher-pressure fluctuation. Other than that, in a system with oscillating flow, increasing the distance between orifices can lead to constructive interference of pressure waves, amplifying pressure fluctuations. The higher $P/\rho gZi$ is a result of the superposition of pressure waves reflecting and forth between the orifices. This is because if the orifices are positioned too closely, there is a risk of interference, resulting in destructed airflow patterns. Sufficient spacing is essential to prevent turbulence and ensure a continuous, smooth flow of air through each individual orifice. This can be supported from the findings by Jingbin et al. (2015) [21].

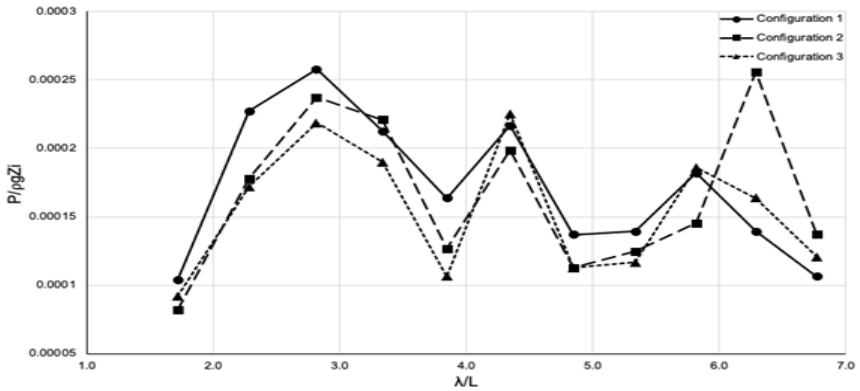

Figure 6. The pressure amplitude

It's proven that having a further distance between orifices increases the $P/\rho gZi$, hence a higher efficiency. Sufficient spacing is essential for enhancing the pressure differentials generated within the chamber as water oscillates. This, consequently, plays an important factor in maximizing the potential energy for efficiency.

*Corresponding Author | Saad, M. R. | rashdan@upnm.edu.my

3.2 Flow Rate at The Nozzle Outlet

According to Figure 7, the three top panels exhibit a similar trend and trajectory. All panels experience a rapid escalation in efficiency from λ/L = 1.7 to 2.8, followed by a steep decline until λ/L = 3.8. However, there is a significant sharp increase in flow rate for all top panels. During the first peak, Configuration 3 achieves the highest flow rate at 0.1378 m^3/s, surpassing Configuration 2 (0.1374 m^3/s) by a minimal difference of 0.29%. Once again, Configuration 2 has the highest flow rate during the third peak at λ/L = 5.8 to 6.3. In contrast, Configuration 1 consistently experiences the lowest flow rate across all three peaks. Although Configuration 3 has the highest flow rate, it also experienced the lowest $P/\rho gZi$. The same can be said for Configuration 1 where it experienced the opposite effect from Configuration 3. The increased in the distance causes the flow to separate from the walls of the water column between the orifices, resulting in regions of recirculating flow. This separation increases resistance and reduces the effective flow area, decreasing the overall flow rate.

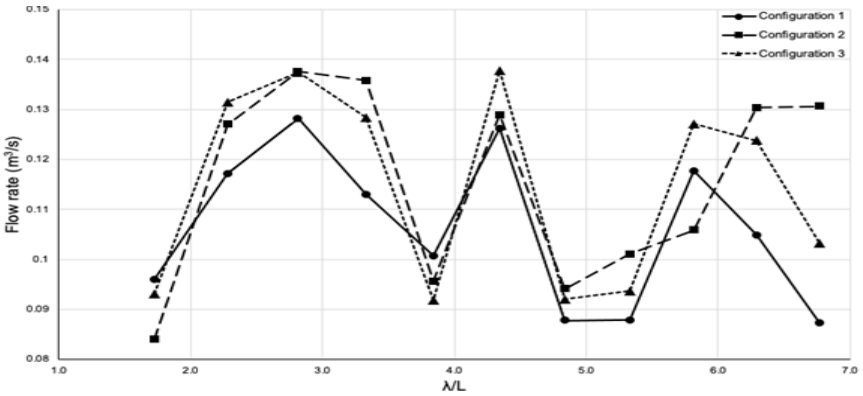

Figure 7. The flow rate output

Other than that, having larger distance between orifices allows for more development of a non- uniform velocity profile between orifices, which can lead to zones of low velocity and high pressure, contributing to higher pressure amplitudes but also reducing the overall flow rate. Thus, it can be said that the pressure amplitude is inversely proportional to the flow rate.

3.3 Primary Conversion Efficiency of The Device

Based on the observations from Figure 8, all three top panels exhibit a similar trend line, reaching their peak efficiency at λ/L=2.8. Afterward, there is a sharp decline in efficiency for all three panels from λ/L = 2.8 to 3.8, followed by an increase again at λ/L = 4.3. Configuration 1 achieves the highest efficiency of 0.092%, closely followed by Configuration 2 at 0.091%, with a minimal discrepancy of 1.09%. However, during the period of λ/L = 3.8 to 4.3, Configuration 3 outperforms the other top panels in terms of efficiency. It is crucial to highlight that during low λ/L periods, the efficiencies are higher and decrease as λ/L increases. Therefore, it is proven that BBDB suits Malaysia's low heave wave conditions.

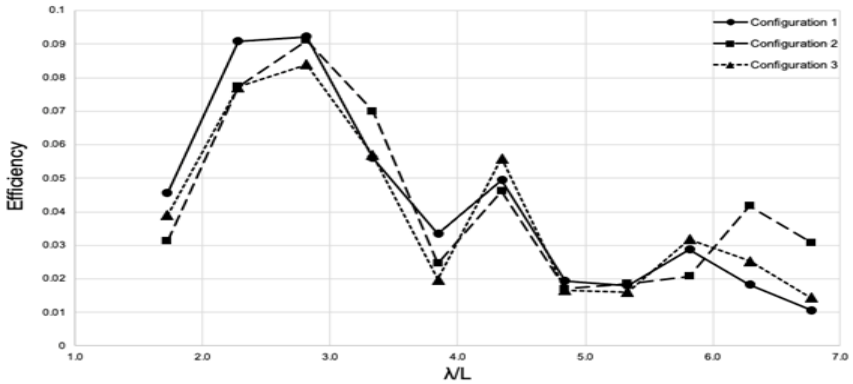

Figure 8. The primary conversion efficiency

*Corresponding Author | Saad, M. R. | rashdan@upnm.edu.my

4.0 CONCLUSION

In terms of efficiency, Configuration 1 stands out with the highest performance, surpassing Configuration 2 by a notable difference of 1.09%. However, when considering flow rates, Configuration 3 takes the lead with the highest flow rate, while Configuration 1 exhibits the lowest flow rate among all configurations. Whereas for pressure amplitude, Configuration 1 attained the highest amplitude, followed closely by Configuration 2. Interestingly, Configuration 2 appears as the second-highest performer, not only in flow rate but also in pressure amplitude and efficiency. The low in efficiency of this device is mainly caused by the shallow water conditions, which limit its ability to perform effectively. The scope of this research solely focuses on the primary conversion efficiency, specifically within shallow water conditions. It should be noted that the study does not fully capture a real ocean wave condition. To enhance the future investigations, it is recommended to conduct experiments in deep water conditions, allowing for a more accurate simulation of actual oceanic environments. For future research, it is recommended to adopt a design like Configuration 1 as it gave out the highest efficiency during this experiment. Despite these acknowledged limitations, the findings of this study remain valuable and can serve as a useful reference for researchers exploring similar domains.

5.0 CONFLICT OF INTEREST

The authors declare no conflicts of interest.

6.0 AUTHORS CONTRIBUTION

Mohd Azhar, N. A. (Methodology; Formal analysis; Data curation; Formal analysis; Investigation; Writing - original draft; Writing - review & editing)
Omar, M. A. (Methodology; Formal analysis)
Abdul Rahman, M. R. (Conceptualisation; Methodology; Resources; Software; Writing - review & editing; Funding acquisition; Supervision)
Mukhtar, A. (Conceptualisation; Methodology; Validation; Resources; Writing - review & editing; Funding acquisition; Supervision)
Samion, M. K. H. (Methodology; Data curation; Resources)
Imai, Y. (Conceptualisation; Methodology)
Saad, M. R. (Conceptualisation; Methodology; Resources; Writing - review & editing; Funding acquisition; Project administration; Supervision)

7.0 ACKNOWLEDGEMENTS

This research received support from Joint Research/Usage for Institute of Ocean Energy Saga University Japan 2023 (Acceptance No: 23B09). The authors would also like to extend their gratitude to National Defence University of Malaysia for sponsoring the project through the Graduate Research Assistant Fellowship under the PPPI Trust Fund UPNM.

List of Reference

[1] Lelieveld, J., Klingmüller, K., Pozzer, A., Burnett, R. T., Haines, A., & Ramanathan, V. (2019). Effects of fossil fuel and total anthropogenic emission removal on public health and climate. *Proceedings of the National Academy of Sciences*, *116*(15), 7192-7197.
[2] Zevenhoven, R., & Beyene, A. (2011). The relative contribution of waste heat from power plants to global warming. *Energy*, *36*(6), 3754-3762.
[3] Pelc, R., & Fujita, R. M. (2002). Renewable energy from the ocean. *Marine policy*, *26*(6), 471-479.
[4] Dincer, I. (Ed.). (2018). *Comprehensive energy systems*. Elsevier.
[5] Aderinto, T., & Li, H. (2018). Ocean wave energy converters: Status and challenges. *Energies*, *11*(5), 1250.
[6] Withers, T., & Neill, S. (2021). Salinity Gradient Power. In *Earth Systems and Environmental Sciences*. Elsevier Press.
[7] Drew, B., Plummer, A. R., & Sahinkaya, M. N. (2009). A review of wave energy converter technology.
[8] Zhang, D., Li, W., & Lin, Y. (2009). Wave energy in China: Current status and perspectives. *Renewable energy*, *34*(10), 2089-2092.
[9] McCormick, M. E. (2013). *Ocean wave energy conversion*. Courier Corporation.

*Corresponding Author | Saad, M. R. | rashdan@upnm.edu.my

[10] Dolores, E. M., José, S. L. G., & Vicente, N. (2017). Classification of wave energy converters. *Recent Advances in Petrochemical Science*, *2*(4), 555593.
[11] Astariz, S., & Iglesias, G. (2015). The economics of wave energy: A review. *Renewable and Sustainable Energy Reviews*, *45*, 397-408.
[12] Pietra, L., Tello, M., Bhattacharjee, J., & Soares, C. G. (2012). Review and classification of wave energy converters. *Centre for Marine Technology and Engineering (CENTEC), Instituto Superior Técnico, Lisboa, Portugal. doi*, *10*.
[13] Yemm, R., Pizer, D., Retzler, C., & Henderson, R. (2012). Pelamis: experience from concept to connection. *Philosophical Transactions of the Royal Society A: Mathematical, Physical and Engineering Sciences*, *370*(1959), 365-380.
[14] Jozanović, B. (2021). *Energetske Karakteristike Postrojenja Na Morske Valove* (Doctoral dissertation, Josip Juraj Strossmayer University of Osijek. Faculty of Electrical Engineering, Computer Science and Information Technology Osijek. Department of Power Engineering. Chair of Power Plants and Energy Processes).
[15] Heath, T. V. (2000, January). The development and installation of the LIMPET Wave Energy Converter. In *World renewable energy congress VI* (pp. 1619-1622). Pergamon.
[16] Joubert, J. R., van Niekerk, J. L., Reinecke, J., & Meyer, I. (2013). Wave energy converters (WECs). *CRSES: Matieland, South Africa*.
[17] Aiman, M. J., Ismail, N. I., Saad, M. R., Imai, Y., Nagata, S., Samion, M. K. H., ... & Rahman, M. R. A. (2020). Study on shape geometry of floating oscillating water column wave energy converter for low heave wave condition. *Journal of Advanced Research in Fluid Mechanics and Thermal Sciences*, *70*(2), 124-134.
[18] Imai, Y., Toyota, K., Nagata, S., Setoguchi, T., Oda, J., Matsunaga, N., & Shimozono, T. (2008, January). An experimental study of negative drift force acting on a floating OWC "backward bent duct buoy". In *International Conference on Offshore Mechanics and Arctic Engineering* (Vol. 48203, pp. 871-879).
[19] Imai, Y., Toyota, K., Nagata, S., & Mamun, M. A. (2010). Duct extension effect on the primary conversion of a wave energy converter 'backward bent duct buoy'. *OTEC/佐賀大学理工学部附属海洋熱エネルギー変換実験施設, 佐賀大学理工学部編*, *15*, 33-36.
[20] Elhanafi, A., Macfarlane, G., Fleming, A., & Leong, Z. (2017). Experimental and numerical investigations on the hydrodynamic performance of a floating–moored oscillating water column wave energy converter. *Applied energy*, *205*, 369-390.
[21] Jingbin, L., Gensheng, L., Zhongwei, H., & Xianzhi, S. (2015). A Study About the Effect of the Structure Parameters of the Multi-Orifices Nozzle on Nozzle Discharge Coefficient. *2015 WJTA Conference and Expo.*

*Corresponding Author | Saad, M. R. | rashdan@upnm.edu.my